

# **An In-Situ Test Method for Evaluating the Coupled Pore Pressure Generation and Nonlinear Shear Modulus Behavior of Liquefiable Soils**

Brady R. Cox <sup>1</sup>, Kenneth H. Stokoe, II <sup>2</sup>, and Ellen M. Rathje<sup>3</sup>

<sup>1</sup>Assistant Professor, Department of Civil Engineering, University of Arkansas, 4190 Bell Engineering Center, Fayetteville, AR 72701; brcox@uark.edu

<sup>2</sup>Jennie C. and Milton T. Graves Chair, Professor, Department of Civil, Architectural, and Environmental Engineering, University of Texas, 1 University Station C1792, Austin, TX 78712; k.stokoe@mail.utexas.edu

<sup>3</sup>Associate Professor, Department of Civil, Architectural, and Environmental Engineering, University of Texas, 1 University Station C1792, Austin, TX 78712; e.rathje@mail.utexas.edu

**Abstract:** An in-situ test method for evaluating the coupled response between excess pore water pressure generation and nonlinear shear modulus behavior has been developed. This technique is an active, strain-based method that may be used to directly evaluate the liquefaction resistance of soils in place. The test is based on the premise of dynamically loading a native soil deposit in a manner similar to an earthquake while simultaneously measuring its response with push-in sensors. Dynamic loading is performed via a large, buggy-mounted hydraulic shaker (vibrois) that is used to generate vertically propagating (downward), horizontally polarized shear waves ( $S_{vh}$ -waves) of varying amplitude within an instrumented portion of a liquefiable soil deposit. The newly-developed, push-in sensors consist of a three-component (3D) MEMS accelerometer and a miniature pore water pressure transducer. The new test method has been used to conduct field experiments in liquefiable soil deposits approximately 3 to 4 m below the ground surface. These tests were successful at measuring: (1) excess pore water pressure generation, and (2) nonlinear shear modulus behavior in native silty-sand deposits as a function of induced cyclic shear strain and number of loading cycles. These accomplishments represent a large step forward in the ability to accurately evaluate the susceptibility of a soil deposit to earthquake-induced liquefaction. While typical test results are presented herein, this article primarily focuses on the equipment, field testing practices, and data analysis procedures for the new test method.

**Keywords:** field testing, liquefaction, pore pressure, shear modulus, shear strain

## **Introduction**

It is well established that loose, dry, granular soils tend to densify under both static and cyclic loadings. If these same soils are saturated and then subjected to undrained loading, the tendency to densify causes a buildup of pore water pressure, which in turn reduces the contact stresses between individual soil particles, thus reducing the strength and stiffness of the soil. Rapid earthquake loading often triggers excess pore water pressure generation in loose, saturated soil deposits. When the pore water pressure approaches a value equal to the effective overburden pressure, the soil weakens to a point where it is said to have liquefied (Seed and Idriss 1982). Earthquake-induced soil liquefaction can cause a diverse range of geotechnical problems, including differential settlement and bearing capacity failures of buildings, slope failures of earth dams, lateral spreads and landslides, and floatation of buried pipes and tanks.

The state of the practice for evaluating the susceptibility of soil deposits to liquefaction is centered around simplified procedures based either on direct measurements of pore pressure generation in cyclic laboratory tests (Seed and Idriss 1971; Dobry et al. 1982) or indirect empirical correlations derived from various in-situ tests (Youd et al. 2001). Unfortunately, these procedures have disadvantages related to sample disturbance/representation when laboratory testing is involved, and their indirect nature when empiricism is used. A more robust approach to the problem of evaluating liquefaction susceptibility would involve directly measuring the pore pressure generation characteristics and nonlinear shear modulus behavior of the soil in situ under cyclic loading.

During an earthquake, the generation of excess pore water pressure in a soil mass is directly related to the amplitude and number of shear strain loading cycles (Dobry et al. 1982; Vucetic and Dobry 1986). However, at this time, no active field test methods are available that can be used to directly measure the excess pore pressure generation and nonlinear shear modulus behavior of in-situ soils as a function of induced cyclic shear strain. While blasting has proven to be an effective tool for liquefying soils (Charlie et al. 1992; Gohl et al. 2001), issues regarding the high frequency content and extreme ground accelerations associated with blast-induced liquefaction make it a difficult tool to use when trying

to systematically analyze the potential a soil has to strain and buildup pore pressure during an earthquake. In-situ measurements of both dynamic soil response and pore pressure generation during earthquakes have been reported (Ishihara et al. 1981; Ishihara et al. 1989; Shen et al. 1991; Holzer et al. 1989; Youd and Holzer 1994). In these studies, classified as passive measurements, instrumentation was installed and researchers waited for an earthquake to load the site. Despite efforts to make these types of measurements for more than 25 years, only limited amounts of data have been collected at a few select sites around the world. While these measurements represent the ultimate field investigation of liquefaction potential, they have several key limitations: (1) the unknown recurrence of earthquakes (hence, potentially decades of waiting), (2) the durability of the sensors after long waiting periods, and (3) the inability to perform parametric studies.

This article describes the development and implementation of a new in-situ liquefaction testing technique that can be used for evaluating the coupled response between excess pore water pressure generation and nonlinear shear modulus behavior. The test is based on the premise of dynamically loading a native soil deposit in a manner similar to an earthquake while simultaneously measuring its response with push-in sensors. Dynamic loading is performed via a large, buggy-mounted hydraulic shaker (vibroiseis) that is used to generate vertically propagating (downward), horizontally polarized shear waves ( $S_{vh}$ -waves) of varying amplitude within an instrumented portion of a liquefiable soil deposit. Newly-developed, push-in sensors consisting of a three-component (3D), Micro-Electrical Mechanical Systems (MEMS) accelerometer and a miniature pore water pressure transducer (PPT), are installed from the ground surface in a two-dimensional (2D), trapezoidal array within the liquefiable soil layer and are retrievable upon completion of testing.

Work on this new in-situ liquefaction test is currently in its second stage of development. In the first stage, liquefaction of large-scale, reconstituted, test specimens was accomplished (Chang 2002; Rathje et al. 2004; Stokoe et al. 2004; Rathje et al. 2005; Chang et al. 2007). These tests were successful in evaluating the cyclic threshold shear strain of shallow (depths less than 1.5 m), reconstituted soil deposits, using Rayleigh-type surface waves for dynamic loading. Building on the success of the first-

generation testing, it was desired to advance the technique to a second-generation level by extending the measurements to natural soil deposits and greater depths, implementing the use of vertically propagating shear waves for dynamic loading, evaluating the nonlinear shear modulus behavior of the soil, and quantifying the degradation of the nonlinear shear modulus due to the generation of excess pore pressure.

The second-generation test was used to conduct field experiments at the Wildlife Liquefaction Array (WLA) in Imperial Valley, California. WLA has been intensely studied over the past 25 years (Bennett et al. 1984; Bierschwale and Stokoe 1984; Hagg and Stokoe 1985; Vucetic and Dobry 1986; Youd and Bartlett 1988; Holzer et al. 1989; Dobry et al. 1989; Dobry et al. 1992; Hushmand et al. 1992; Youd and Holzer 1994; Zeghal and Elgamal 1994). It has also recently been designated as a Network for Earthquake Engineering Simulation (NEES) site for the study of soil liquefaction (<http://nees.ucsb.edu>). The extensive site characterization, the documented occurrence of earthquake-induced soil liquefaction at the site twice in the 1980's (1981,  $M_w = 5.9$  Westmorland earthquake; and 1987,  $M_w = 6.6$  Superstition Hills earthquake) and the likelihood for re-liquefaction of the site during subsequent earthquakes made WLA an ideal location for evaluating the proposed in-situ dynamic liquefaction test method.

In-situ tests were conducted in a liquefiable soil deposit approximately 3 to 4 m below the ground surface at WLA. The tests were successful at measuring: (1) excess pore water pressure generation, and (2) nonlinear shear modulus behavior in the native silty-sand deposits as a function of induced cyclic shear strain and number of loading cycles. While typical test results are presented herein, this article primarily focuses on the equipment, field-technique and data analysis procedure for the new test method. Detailed test results and comparisons to pore pressure generation and nonlinear shear modulus curves previously developed for WLA soils from laboratory testing methods may be found in Cox (2006).

### **Methodology of In-Situ Liquefaction Test**

A schematic of the testing configuration is shown in Figure 1. Generally speaking, the vibroseis is used to apply horizontal (in-line) excitation at the ground surface. These vibrations primarily create  $S_{vh}$ -waves that travel downward through the instrumented portion of the soil mass. Testing is conducted

in a staged manner in which waves of successively larger amplitudes are generated. A 2D trapezoidal array of push-in liquefaction sensors is used to monitor the response of the soil to these waves. Measurements from each sensor are used to calculate the cyclic shear strain induced in the instrumented portion of the soil mass and determine the associated excess pore water pressure generation and nonlinear shear modulus behavior.

### *Equipment and Instrumentation*

The major components of the in-situ liquefaction test equipment and instrumentation are: (1) the dynamic source, (2) the liquefaction sensors, and (3) the data acquisition system used to power the sensors and record their output signals. Each of the major components of the in-situ liquefaction instrumentation system is discussed in detail below.

Dynamic Source. The dynamic source employed in this testing is the triaxial vibroseis (affectionately named “T-Rex”) operated by the George E. Brown, Jr. Network for Earthquake Engineering Simulation (NEES) field equipment site at the University of Texas at Austin (nees@UTexas; <http://nees.utexas.edu>). T-Rex is shown in the schematic of Figure 1. The force output of T-Rex in the horizontal mode is about 133 kN and decreases at frequencies below 5 Hz. It also has an adjustable hold-down force for applying variable surface stresses and a CPT-type hydraulic ram to aid in sensor installation and extraction. For in-situ liquefaction tests, T-Rex was operated in the horizontal in-line direction of vibration, thus generating strong shear waves traveling downward from the ground surface polarized in line with the direction of the vehicle and the liquefaction sensor array.

Liquefaction Sensors. Soil liquefaction is a complex phenomenon involving the coupled response of the soil skeleton and pore water. Therefore, a sensor used to track the soil liquefaction process must also couple the ability to simultaneously record soil particle motion and pore water pressure generation (Stokoe et al. 2004). The in-situ liquefaction sensor that was designed and constructed for this research is shown in Figure 2. The sensor is compact, measuring 12.7 cm from tip-to-top and 3.8 cm in diameter, with an approximate unit weight of  $14.1 \text{ kN/m}^3$ . The main body of the sensor, where the

instrumentation is housed, is a cylindrical, acrylic case with a 60-degree conical tip. It has an aluminum top piece that protects the acrylic main body from the heavy, steel push rods and keeps the sensor oriented during installation. The electrical cable contains six-pairs of individually twisted and shielded conductors that power the instrumentation and carry their signals back to the ground surface. Its polyurethane cable jacket is extremely tough, flexible, and waterproof. Because the sensor must be detached from the push rods prior to dynamic loading, it is also equipped with a flexible, small diameter (0.24 cm), stainless steel wire rope that allows it to be pulled out of the ground upon completion of testing. The wire rope is attached to an extraction hook on the outside of the sensor so that it can easily be removed or replaced if broken. The sensor houses a 3D MEMS accelerometer and miniature PPT with a porous bronze filter.

MEMS accelerometers are capacitance-based transducers that, unlike traditional accelerometers, have the ability to sense and respond to both static (gravity) and dynamic accelerations. MEMS accelerometers were chosen for the vibration-sensing component of the liquefaction sensor because of: (1) their compact size, (2) their high output at low frequencies of vibration, (3) their ability to track tilt of the sensor as it is pushed into place, and (4) their ability to monitor any tilt of the sensor that might occur during liquefaction testing. The MEMS accelerometer that was ultimately selected for use in the in-situ liquefaction sensors is a Silicon Designs model 2430-002. It is a triaxial sensing device with an output of 2.5 volts per g. Its nominal three-decibel frequency range is 0 to 300 Hz, and it has a full-scale amplitude range of  $\pm 2g$ . The 3D-MEMS accelerometers were calibrated statically for tilt response and dynamically for amplitude and phase response before use.

PPT's are needed to measure both the static and dynamic response of the pore water during in-situ liquefaction testing. Two different types of PPT's were employed in this research. One of them is a miniature model that is integrated into the liquefaction sensors (Figure 2), while the other is a larger, more stable model housed in its own acrylic case without a vibration sensing device. During testing, the liquefaction sensors occupied nodes #1 through #4 in the trapezoidal array (Figure 1), while the slightly larger pressure transducer occupied node #5 at the center of the array.

The miniature PPT used in all of the in-situ liquefaction sensors is an Entran model EPX-V02-

25P. This PPT is a sealed-reference pressure transducer with a nominal output of 0.3 mV per kPa and a 172 kPa range. Its primary advantage is its compact size (just over 2.5 cm long), which allows it to be integrated into the liquefaction sensors so that ground motion and pore pressure can be measured at the same location. However, miniature-type PPT's have a tendency to drift, particularly right after they are powered-up. Additionally, their zero offset value (i.e. voltage output at atmospheric pressure) may change substantially every time they are re-powered (it should be noted here that Druck model PDCR-81 miniature PPT's were also experimented with in this research and found to have the same problems). Nevertheless, based on multiple calibrations in the laboratory and in the field, the drift phenomenon and shifting zero offset were not found to affect dynamic sensitivity (i.e. relative change in voltage as a function of the change in pressure) of the miniature PPT's. Despite large fluctuations in zero offset, the slopes of the pressure calibration results remained quite steady (within 2% of the mean slope values). This evidence showed that the miniature PPT's could be used to make accurate dynamic (excess) pressure measurements despite their inability to accurately resolve the absolute (static) water pressure.

A larger, more stable pressure transducer was desired as a reference standard for static pressure readings. The Druck model PDCR 35/D was chosen for this application. It is approximately 10.2 cm in length and 1.0 cm in diameter. The version with a 69 kPa range was selected for this study. It has a nominal output of 1.4 mV per kPa and was found to be extremely stable both statically and dynamically. Because of its stable and reliable nature, the PDCR 35/D was the primary PPT used in all of the quantitative in-situ liquefaction test data processing. The dynamic pressure data obtained from the miniature PPT's, while believed to be quite accurate, were only used in a qualitative sense to observe how pore pressure generation and dissipation varied throughout the array.

When attempting to make dynamic pore pressure measurements, time lags and amplitude decay of the PPT signal may be caused by a relatively low permeability filter, a filter smeared or clogged with soil, a partially saturated filter, or air trapped in the cavity between the pressure-sensing diaphragm and the filter (Chang 2002; Dunnycliff 1988). The permeability of the filter should be fine enough to keep the PPT cavity saturated during installation and prevent clogging by fine-grained soil, yet coarse enough to

minimize any time lag or amplitude decay of the dynamic pressure signal.

The filter material used in this study is sintered bronze with nominal pore sizes of 20 microns. This material was chosen based on guidelines presented in ASTM D5778 (Standard Test Method for Performing Electronic Friction Cone and Piezocone Penetration Testing of Soils) and on experience gained from the first-generation of testing (Chang 2002). A pore size of 20 microns is an order of magnitude less than the minimum filter pore size of 200 microns set forth in ASTM D5778. This pore size was found to be fine enough to help maintain saturation and prevent filter clogging during installation, yet coarse enough not to affect dynamic response during testing.

Prior to field testing, the porous filters are saturated by boiling them in water for at least four hours. The filters are then sealed in air-tight containers until they are installed on the sensors in the field. During field testing, the sensor is placed in a bucket of water along with a container of saturated filters. The container is opened under water so that the filters are not exposed to air. Before placing a filter on the sensor, the PPT cavity is visually inspected to make sure that no air bubbles are trapped inside. After the filter is secured to the sensor, a tightly-fitting rubber membrane is placed around the sensor while still under water. Once the membrane is on, the sensor can be removed from the bucket and oriented on the push rod for installation.

Data Acquisition. The output signals from the liquefaction sensors were recorded using a 72-channel dynamic signal analyzer that has VXI hardware and Data Physics software. During field testing, fixed frequencies of 10 and 20 Hz were used to dynamically load the soil in shear by driving the vibroseis (T-Rex) with an external function generator. The sensor outputs from these tests were recorded at a constant sampling rate of 8192 samples per second ( $\Delta t = 0.12$  ms). While this sampling rate may be considered as oversampling in terms of frequency domain measurements, it was chosen so that enough data points would be digitized in the time domain to allow accurate determination of the shear wave time lag (phase difference) between the upper and lower layer of liquefaction sensors in the trapezoidal array.

Typically, 100 cycles of dynamic loading were applied to the soil deposit. Despite the fact that dynamic loading lasted for ten seconds or less, it was desired to record continuous blocks of data up to

120 seconds long to capture the complete trend of pore water pressure generation and subsequent dissipation. The data recorded included: (1) the vibroseis drive signal from the function generator, (2) the ground force signal from the vibroseis truck, (3) the PDCR 35/D pressure transducer output signal, and (4) a total of 16 output signals from four separate liquefaction sensors (one miniature PPT signal and three components of vibration from the MEMS accelerometer in each liquefaction sensor).

### *Test Procedure*

The generalized in-situ liquefaction test procedure may be subdivided into three basic categories. They are: (1) sensor installation, (2) staged dynamic loading, and (3) sensor extraction.

Sensor Installation. The liquefaction sensors are installed with the aid of heavy-walled, hollow, steel push rods (outside diameter 3.8 cm) and a CPT-type hydraulic cylinder located on the back bumper of T-Rex. Prior to sensor installation, a slightly oversized (4.4-cm diameter), steel pilot cone is typically pushed to a depth just below the ground water level (GWL) and then removed. The oversized cone is used to create a pilot hole, which serves two purposes: (1) it prevents the sensor from being damaged while penetrating a stiff surface crust, and (2) it allows the sensor to be placed below the GWL with the saturation membrane still in place. The oversized pilot cone should not be pushed too close to the liquefiable layer, as this will create a void around the push rods that water can readily escape through during the test.

As discussed above, an electrical cable and a wire rope are attached to each liquefaction sensor. These members pass through the hollow section of the push rods until they reach the ground surface. The electrical cable and wire rope fill most of the space inside the hollow rods. However, to ensure that ground water will not escape through the hollow section of the push rods during dynamic loading, a tapered rubber gasket is placed around the cables just above the sensor connection. Vacuum grease is placed around the cables in the vicinity of the gasket to help seal the plug and provide sliding lubrication when the sensor is decoupled from the push rods.

The sensor and push rod are coupled together via a simple compression fit. Small cylindrical

grooves in the aluminum top piece of the sensor mate with pins inside the hollow push rod to keep the sensor oriented during installation. After the sensor is oriented on the push rod, it is lowered by hand down the oversized pilot hole to a temporary resting place just below the GWL. Note that the pilot hole begins in a shallow trench just below the ground surface. A trench is needed because the liquefaction sensor cables and the tops of the push rods must be below the ground surface so the base plate of T-Rex does not come into contact with them during dynamic loading.

After the sensor has been placed below the GWL, the hydraulic ram is used to push it through virgin soil to its pre-selected location. The thin rubber membrane is torn from the sensor as it is pushed into place. After the sensor is in place, the push rod is decoupled from the sensor by withdrawing it a short distance (approximately 8 cm). During this process, the relative movement between the push rods and the sensor cable is monitored to make sure that the sensor stays in place. This withdrawal helps to ensure that the dynamic movement of the sensor will not be influenced by the presence of the heavy push rods. However, the push rods remain in the hole to prevent water from escaping during dynamic loading. A square metal bracket is threaded onto the top of the push rods to keep them from slipping back down the hole and coming into contact with the sensor.

The sensors are installed one at a time, forming a linear, 2D array beneath the ground surface. The final positions of the sensors are known quite precisely, as the relative movement between the sensor cable and the push rod is monitored during decoupling. Additionally, the tilt of each liquefaction sensor is tracked using the 3D MEMS accelerometer. This allows the positions (horizontal and vertical) of the sensors to be updated if necessary using the measured tilt angles and the length of the push rod. A picture of a completed sensor array, as viewed from the in-line direction at the ground surface, is shown in Figure 3. The numbers next to each liquefaction sensor do not represent the order in which they were installed, but rather their positions in the array (Figure 1). The corner sensor positions may be considered as nodes of a single quadrilateral element. This configuration allows the shear strains anywhere within the element to be calculated as a function of the displacements sensed at each of the nodes. As strains are most often calculated at the center of the element, the stable PDCR 35/D pressure transducer is placed in position #5

so that the calculated shear strains can be coupled with precise measurements of static and dynamic pore water pressure.

While not ideal, the push rods must be left in place to ensure that the sensors can be retrieved upon completion of testing, and to prevent a ready path for pore pressure dissipation during testing. The rods certainly stiffen the overlying soil to some unknown extent. However, with the exception of the rod used to install sensor #5, the push rods are outside of the soil mass where shear strain, pore pressure, and shear modulus measurements are taking place. Close agreement between in-situ test results and published laboratory test results (pore pressure generation and nonlinear shear modulus curves) for Wildlife soils support the fact the influence of the push rods is minor (Cox 2006).

After all sensors have been installed, two crosshole source rods are inserted in line with the array (Figure 3). They are placed just far enough away from the sensor array so that they will be out from under the base plate of T-Rex during dynamic loading. One is inserted so that its tip is located at approximately the same elevation as sensor #1 and #2, while the other is inserted coincident with the elevation of sensor #3 and #4. This configuration allows small-strain crosshole seismic tests to be performed between each pair of sensors before and after dynamic loading. During crosshole testing, compression wave (P-wave) velocities and shear wave ( $S_{hv}$ -wave, horizontally propagating, vertically polarized shear wave) velocities are measured using interval travel times. The most important reason for making P-wave velocity measurements is to verify the saturation level of the liquefiable material. While beyond the scope of this paper, it should be noted that one of test locations at WLA was found to be only partially saturated despite being several meters below the GWL. The lack of complete saturation manifested some very interesting results in terms of cyclic threshold shear strain and subsequent pore pressure generation (Cox 2006).

After the sensors and crosshole source rods have been installed, the trench is backfilled with loose soil, and T-Rex is brought into position with its base plate directly over the center of the instrumentation array. The base plate of T-Rex is 2.3 m x 2.3 m, while the maximum horizontal extent of the liquefaction array is only 1.2 m (Figure 1). Therefore, the base plate completely covers the vertical projection of the

sensor array. A static hold-down force is applied to the base plate to keep it coupled to the ground during dynamic loading, which increases the state of stress in the instrumented soil deposit. It is important to know how the state of stress is altered so that it can be taken into account in the data reduction process. The uniform surface pressure (assuming the base plate to be rigid) applied by the base plate during testing was approximately 38 kPa, which corresponds to the maximum hold-down force of T-Rex.

Staged Dynamic Loading. During dynamic loading, T-Rex is used to excite the instrumented soil mass in shear by driving the base plate horizontally in line with the array, thus generating strong shear waves that propagate downward through the sensor array. To evaluate in-situ pore pressure generation curves and nonlinear shear modulus behavior, a wide range of cyclic shear strains need to be induced within the instrumented soil mass. A staged dynamic loading sequence is used to generate the wide strain range.

At the beginning of the dynamic test sequence, the vibroseis is driven at its lowest possible output. A typical dynamic load used during field testing is 100 cycles of a 10- or 20-Hz fixed sine wave. After this excitation is applied, the recorded data is monitored to ensure no excess pore pressure is generated. Then, the dynamic load is applied again at a slightly larger amplitude. In this manner, shear strain within the soil mass is sequentially elevated until a small amount of excess pore pressure is measured. This indicates that the shear strain induced in the instrumented portion of the soil deposit has just surpassed the cyclic threshold strain ( $\gamma_i^c$ ). At this point, the test is paused while the excess pressure is allowed to dissipate. When the pressure comes to equilibrium at its hydrostatic value, staged testing is resumed. However, at this point the vibroseis is generally driven at its maximum output to avoid repetitive staged loading beyond the cyclic threshold shear strain.

Sensor Extraction. After staged dynamic loading, the liquefaction sensors must be extracted. Because the push rods are decoupled from the sensors during installation, a pre-attached wire rope is used to pull them out of the ground. This process is made somewhat easier by withdrawing the push rods from the hole simultaneously with the sensor. Even though the sensor and the rods are not physically

connected together, the rods help to keep the hole from collapsing too far ahead of the sensor. This reduces the stress placed on the sensor and minimizes the chance of breaking the wire rope.

### **Data Analysis for the In-Situ Liquefaction Test**

The raw data recorded during the in-situ liquefaction test consists of acceleration and pore water pressure time histories at each sensor location. The processed data desired from the test are: (1) induced cyclic shear strain, (2) excess pore water pressure ratio as a function of induced cyclic shear strain and number of loading cycles, and (3) nonlinear soil shear modulus as a function of induced cyclic shear strain and change in pore water pressure. The analytical techniques used to produce this information are discussed below.

#### *Raw Data Processing*

After the raw output voltages from the accelerometers have been converted into units of acceleration via calibration factors, the acceleration time histories are numerically integrated once to obtain velocity time histories, and twice to obtain displacement time histories. Numerical integration is performed in the time domain using the trapezoidal rule. Baseline correction to remove drift in the integrated signals was performed in the frequency domain by high-pass filtering. A cut-off frequency of 2 Hz was used, as there was no evident energy in the original raw accelerometer data at frequencies below this value. The displacement time histories are of primary interest in the subsequent shear strain evaluation procedures.

#### *Shear Strain Evaluation*

The data collected during in-situ liquefaction tests allow shear strains induced in the instrumented portion of the soil to be calculated in several different ways. The two primary shear strain evaluation methods can be categorized as: (1) displacement-based (DB), and (2) wave propagation-based (WB) (Rathje et al. 2005). DB shear strain evaluation methods use the displacement time histories at each liquefaction sensor and the relative distances between sensors to evaluate shear strain time histories. WB

shear strain evaluation methods use the ratio of the particle velocity time histories at each sensor and the strain-dependant shear wave velocity measured between sensors to evaluate shear strain time histories. It was found that the DB method gave more reliable results for the test setup used in this research. The WB method tends to under predict the shear strain induced in the array because it does not take into account the vertical particle motion caused by rocking of the vibroseis base plate. Therefore, only the DB method will be discussed further herein. Detailed comparisons of DB and WB shear strains calculated from in-situ liquefaction test data may be found in Cox (2006), Rathje et al. (2005), Rathje et al. (2004), and Chang (2002).

As discussed above, the corner positions in the sensor array may be considered as nodes of a single, quadrilateral element. This configuration allows the strains anywhere within the element to be calculated from the displacements at the sensors (nodes) using a 4-node, isoparametric finite element formulation (Rathje et al. 2004, 2005). For an in-situ liquefaction test, the vertical ( $z$ ) and horizontal in-line ( $y$ ) components of particle displacement at each sensor location are used to calculate the in-plane shear strain ( $\gamma_{yz}$ ) induced at the center of the array. An example of a shear strain time history calculated at the center of the trapezoidal array is shown in Figure 4. This shear strain time history was generated by 100 cycles of dynamic loading in the form of a 10-Hz fixed sine wave and has amplitudes close to the theoretical cyclic threshold strain ( $\gamma_t^c \sim 0.02\%$ ). Dynamic in-situ liquefaction tests are not strictly stress-controlled or strain-controlled tests. Nonetheless, the strain time histories calculated at the center of the array generally have very consistent amplitudes over all cycles of excitation throughout much of the staged loading program. For example, the shear strain time history shown in Figure 4 has an average shear strain over the first 10 cycles of 0.023% and an average shear strain over all 100 cycles of 0.029%. However, once significant excess pore water pressures are generated within the array, the strain behavior can become quite irregular. These cases are discussed on an individual basis when specific test results are presented (Cox 2006).

The 4-node, isoparametric finite element formulation provides strain values within the element

that are first-order accurate. The most critical assumption in the method is the linear variation of displacement between nodes (Rathje et al. 2004, 2005). For this assumption to be valid, the size of the array in the direction of wave propagation should be less than about one-quarter of the wavelength of the highest significant frequency (i.e., the shortest wavelength) used during testing (Chang 2002). The highest frequency used during in-situ liquefaction tests was 20 Hz. The liquefiable soil tested in these studies has a shear wave velocity ( $V_s$ ) of approximately 122 m/s. Therefore, a 20-Hz wave propagating through this material would have a wavelength of about 6 m, which is ten times greater than the vertical dimension of the liquefaction sensor array. It is therefore believed that a linear variation of displacement between nodes is a valid assumption for this test setup.

#### *Pore Pressure Ratio Evaluation*

Examples of pore water pressure time histories obtained from the center PPT are shown in Figure 5. Figure 5a shows a pore pressure time history obtained from a test in which shear strains induced in the instrumented soil deposit were not large enough to generate excess pore water pressure ( $\gamma_{yz} \sim 0.012\%$ ). Figure 5b shows a pore pressure time history obtained from a test in which shear strains induced in the instrumented soil deposit were sufficiently large to generate excess pore water pressure ( $\gamma_{yz} \sim 0.027\%$ ). The static water pressure prior to shaking is approximately 20.7 kPa (2.1 m of water) in both records. After vibroseis loading begins, the 10-Hz dynamic signal can clearly be seen in Figure 5b. The 10-Hz dynamic signal is also present in Figure 5a, although its amplitude is smaller. This dynamic portion of the signal is referred to as the hydrodynamic pressure (Chang 2002). The onset of the hydrodynamic portion of the signal can be compared with the accelerometer signals as a check on the proper dynamic response of the PPT. In Figure 5b, the pore pressure time history also includes an increase throughout the duration of dynamic loading. This increase in pressure is referred to as the residual pressure. When dynamic loading stops, the pore water pressure has reached a value of approximately 29.0 kPa (3.0 m of water). The excess pore pressure generated during dynamic loading is the difference between the static and final pore water pressures (i.e. approximately 8.3 kPa or 0.9 m of water).

The residual buildup of excess pore water pressure is of primary interest in liquefaction testing because it decreases the effective stress within the soil mass. The hydrodynamic pressure only affects the instantaneous state of effective stress and hence does not have a lasting impact on the soil stiffness or strength. To effectively evaluate the increase in residual pressure at various times during shaking, the hydrodynamic portion of the signal must be separated from the residual portion of the signal. This separation is most readily accomplished using frequency-domain filtering. The residual pressure components of all PPT signals acquired during in-situ liquefaction testing were obtained by applying a 3-Hz low-pass filter to the excess pore pressure records. The hydrodynamic pressure components (if desired) may be obtained by subtracting the residual pressure component from the original excess pore pressure record.

In regards to evaluating soil liquefaction, pore water pressure data are typically quantified in terms of a pore pressure ratio ( $r_u$ ). Pore pressure ratio values are obtained by normalizing the excess pore water pressure by the initial effective confining pressure acting on the soil. In field studies, the normalizing stress is the initial vertical effective stress (i.e.  $r_u = \Delta u / \sigma_v'$ , where  $\Delta u$  is excess pore water pressure and  $\sigma_v'$  is initial vertical effective stress). The  $r_u$  value helps one visualize how close the buildup in residual pressure has come to completely liquefying the soil. An  $r_u$  value equal to 1.0 (or 100%) means that the excess pore pressure has built to the point where it is equal to the initial vertical effective stress, and the soil is said to have fully liquefied. The normalizing initial vertical effective stress was calculated by superimposing the change in vertical stress at depth due to the applied surface load of the vibroseis base plate onto the preexisting effective vertical overburden stress at each sensor location.

Residual pore water pressure values obtained from all five pressure transducers were used to calculate  $r_u$  values for all stages of the in-situ liquefaction tests. However, the  $r_u$  values used to construct the pore pressure generation curves for each site were obtained solely from the PDCR 35/D transducer located at the center of the array. The  $r_u$  values obtained from the miniature PPT's were only used in a qualitative sense to observe how the pore pressure generation varied within the instrumented soil mass.

### *Nonlinear Shear Modulus Evaluation*

The stress-strain behavior of soil is nonlinear under high-amplitude dynamic excitation (Seed and Idriss 1970; Hardin 1978), and is most often characterized in terms of the variation of shear modulus ( $G$ ) with induced shear strain ( $\gamma$ ). Nonlinear soil shear modulus behavior is commonly measured in the laboratory using cyclic triaxial, cyclic simple shear, cyclic torsional shear, or resonant column tests. Other researchers have obtained in situ estimates of nonlinear soil shear modulus behavior through analysis of earthquake strong-motion records from borehole arrays (e.g., Zeghal and Elgamal 1994; Zeghal et al. 1995).

The shear moduli of soils are generally independent of shear strain amplitude in the small-strain range (i.e. shear strains less than approximately 0.001%, depending on soil type and confining pressure). The small-strain shear modulus is referred to as  $G_{\max}$ . It is common to normalize shear moduli values obtained in the larger-strain range by the small-strain shear modulus  $G_{\max}$  to obtain modulus reduction curves ( $G/G_{\max}$ ). The shear strain value where the soil begins to transition from linear, strain amplitude independent to nonlinear, strain amplitude dependant is termed the elastic threshold strain ( $\gamma_t^e$ ). The soil shear modulus decays in a nonlinear fashion at strains greater than  $\gamma_t^e$ , however the nonlinear behavior is independent of the number of loading cycles applied to the soil until the cyclic threshold strain ( $\gamma_t^c$ ) is surpassed. As a general approximation, the cyclic threshold strain is often considered to have a value of approximately 0.01%. The cyclic threshold strain is marked by the tendency of the soil shear modulus to begin degrading with increasing number of loading cycles applied at a constant shear strain. In saturated soils, the cyclic threshold strain is also revealed as the point where excess pore water pressure generation begins (Dobry 1982).

The shear modulus of a soil deposit can be obtained from its shear wave velocity according to the following equation:

$$G = \rho \cdot V_s^2 \quad (1)$$

where  $G$  = the shear modulus of the soil;  $\rho$  = the mass density of the soil; and  $V_S$  = the shear wave velocity of the soil. The procedure used to make this calculation in the context of the in-situ liquefaction test is illustrated in Figure 6. The horizontal excitation and associated shear waves generated by the vibroseis truck are sensed by the horizontal components of the embedded instrumentation as they propagate through the instrumentation array. The instantaneous shear wave velocity of the instrumented soil mass may be obtained by dividing the vertical distance ( $\Delta z$ ) between sensors by the time lag ( $\Delta t$ ) between the top and bottom sensors. A different  $\Delta t$  may be obtained for each cycle of loading so that degradation, as well as nonlinearity, may be evaluated. This process enables one to track the changes in shear modulus throughout the entire process of in-situ liquefaction testing.

The raw outputs of the in-line components of the MEMS accelerometers were used to calculate the time lag between each sensor pair (i.e. sensors #3 and #2, sensors #4 and #1). Cycle-by-cycle time lags were measured between both the peaks and the troughs of the records. The peak and trough time lags for each sensor pair were then averaged together on a cycle-by-cycle basis to obtain the shear wave velocity within the instrumented soil mass. Examples of the cycle-by-cycle shear wave velocities obtained from records collected during an in-situ liquefaction test are shown in Figure 7. Figure 7a displays cycle-by-cycle shear wave velocities that remain essentially constant throughout loading. The average shear strain induced at the center of the array during this loading stage was approximately 0.009%, which is below the cyclic threshold strain for the liquefiable soil deposit (verified by the fact that there was no excess pore pressure generated in the array). An example of the cycle-by-cycle shear wave velocities obtained from records collected during a higher-strain loading stage is shown in Figure 7b. In this case, the average strain induced at the center of the array was approximately 0.045%, which is beyond the cyclic threshold strain for the liquefiable soil deposit (substantiated by the fact that a pore pressure ratio of approximately 12% was induced at the center of the array after 100 cycles of loading). The cycle-by-cycle shear wave velocities clearly decay throughout the duration of loading for this test. The combined effects of softening due to pore water pressure generation and cyclically loading the soil

beyond its cyclic threshold strain cause this degradation.

The procedure described above assumes that the shear waves propagating through the instrumentation array are plane waves. This assumption is believed to be reasonable because the array is located directly below the rigid base plate. The plane wave assumption may also be verified by comparing the amplitude and phase of the waves detected by the horizontal, in-line components of each sensor located at the same depth. These comparisons showed that the amplitude and phase of the in-line components were generally within 2% and 3.0 degrees, respectively, despite the fact that the sensors were located on opposite sides of the centerline of the base plate. This evidence lends credence to the plane shear wave assumption.

As previously mentioned in the Data Acquisition Section, all records were recorded at a constant rate of 8192 samples per second. This sampling rate was chosen to obtain adequate resolution for determining the time lags between sensors. However, harmonic distortion and noise in some of the raw accelerometer records made it difficult to obtain precise values for the time lags between sensors. For example, assuming a shear wave velocity for the soil of 122 m/s and a vertical distance between sensors of 0.6 m, a sampling rate of 8192 samples per second yields approximately 40 digitized points between wave arrivals. If one were to be off by 4 data points (0.0005 seconds) in determining the time lag between sensors, the estimated shear wave velocity would be off by approximately 10%. This would alter the estimated shear modulus by approximately 20%. Frequency-domain filtering and time-domain integration were experimented with in an attempt to reduce the influence of harmonic distortion and noise in the raw accelerometer records and to isolate the loading frequency. While these efforts made the records look much cleaner, the time lags between sensors were adversely altered. Therefore, the raw accelerometer signals were solely used to obtain estimates of the nonlinear shear modulus behavior during all in-situ liquefaction tests. If the raw accelerometer records were not clean enough to make accurate estimates, the shear modulus values were not reported.

### **Example Results from In-Situ Liquefaction Test**

The in-situ dynamic liquefaction test was used to conduct field experiments at the Wildlife Liquefaction Array (WLA) in Imperial Valley, California. Shallow soil deposits at WLA consist of floodplain sediments that fill an old incised channel of the Alamo River. The uppermost soil layer is a silt to clayey-silt crust that is approximately 2.5-m thick. It is underlain by a liquefiable silty-sand layer approximately 4.3-m thick. Beneath these two floodplain deposits is a stiff, 5.2-m thick clay to silty-clay layer (Bennett et al. 1984). The ground water table at the site is controlled by the Alamo River and is typically found at a depth of about 1.2 m (Holzer et al. 1989). The silty-sand layer has liquefied in two previous earthquakes (1981,  $M_w = 5.9$  Westmorland earthquake; and 1987,  $M_w = 6.6$  Superstition Hills earthquake). Three separate in-situ liquefaction tests were conducted within this liquefiable layer at depths between 3 to 4 m below the ground surface. The average fines content and clay-sized ( $5 \mu\text{m}$ ) particle content in this depth range are 37% and 10%, respectively (nonplastic).

An example of the pore pressure generation curves and the normalized nonlinear shear modulus values obtained at one of the WLA sites is presented in Figure 8. The pore pressure generation characteristics and the nonlinear shear modulus behavior of a liquefiable soil deposit are inseparably linked. Therefore, it is beneficial to view these two types of data in the same figure. Data are shown for 10, 20, 50 and 100 cycles of loading. It is evident that the soil does not generate excess pore water pressure until shear strains greater than  $\gamma_t^c$  have been induced in the soil. The in-situ pore pressure generation curves indicate that  $\gamma_t^c$  depends on the number of shear strain cycles ( $n$ ) and ranges from 0.015% for  $n = 100$  to 0.025% for  $n = 10$ . As expected, the data show that for a given cyclic shear strain above  $\gamma_t^c$ , larger pore pressures are generated with increasing numbers of loading cycles.

The shear modulus of the soil decays in a nonlinear manner until after  $\gamma_t^c$  has been surpassed. After  $\gamma_t^c$  is surpassed, the modulus values decay due to the combined effects of nonlinearity (i.e. the shear strain is increasing with increasing number of loading cycles) and degradation (i.e. the pore pressure is increasing with increasing number of loading cycles). However, practically speaking, significant

modulus degradation was not observed in the data until an  $r_u$  of approximately 5% was induced at the center of the instrumented soil mass.

The maximum  $r_u$  value generated at the center of the array during this set of tests was less than 25% and required 100 cycles of loading. This is an abnormally high number of loading cycles for typical earthquake problems. However, due to the location of the sensors within the liquefiable layer it was necessary to use large numbers of loading cycles to obtain significant excess pore water pressures at the center of the array. In this test, the top of the sensor array was placed 0.9 m below the top of the liquefiable soil layer. Elevated pore pressures measured by the top sensors in the array indicate that the liquefiable soil nearest to the overlying less permeable layer liquefied during high amplitude dynamic loading and isolated the array from larger dynamic motions ( $r_u$  values greater than 90% were measured at the top of the array). In hindsight, it is believed that the sensors should have been placed right at the top of the liquefiable layer, thus allowing larger strains and pore pressures to be measured.

There is not room in the present article to discuss in detail the in-situ test results and their comparison to pore pressure generation models and nonlinear shear modulus curves previously developed for WLA soils from laboratory and field tests. Suffice it here to say that the agreement is very good and additional detailed information may be found in Cox (2006).

## **Conclusions**

In regards to soil liquefaction, the generation of excess pore water pressure in a soil mass is directly related to the amplitude and number of loading cycles of shear strain induced in the soil (Dobry et al. 1982; Vucetic and Dobry 1986). However, at this time, no active field test methods are available to the earthquake engineering profession that can be used to directly measure the excess pore pressure generation and nonlinear shear modulus behavior of in-situ soils as a function of induced cyclic shear strain.

This article has described the development and implementation of a new in-situ liquefaction testing technique that can be used for evaluating the coupled response between excess pore water pressure

generation and nonlinear shear modulus behavior. The test is based on the premise of dynamically loading a native soil deposit in a manner similar to an earthquake while simultaneously measuring its response with push-in sensors. Dynamic loading is performed via a large, buggy-mounted hydraulic shaker that is used to generate vertically propagating (downward), horizontally polarized shear waves ( $S_{vh}$ -waves) of varying amplitude within an instrumented portion of a liquefiable soil deposit.

As a result of this research, several significant accomplishments were made. First, a new in-situ liquefaction sensor was designed and constructed that couples the ability to measure dynamic soil particle motions and pore water pressures. The sensor is lightweight and compact, it can be pushed into position from the ground surface, and it can be extracted from the ground at the end of testing. Second, a field testing technique for conducting in-situ liquefaction tests was established. The field testing technique includes a sensor installation procedure, an effective staged dynamic loading sequence, and a sensor extraction procedure. Third, data analysis techniques for calculating induced cyclic shear strains, excess pore water pressure ratios, and nonlinear shear moduli within the instrumented soil mass have been developed and refined. These measurements allow for in-situ determination of the cyclic threshold shear strain of native soil deposits, as well as the tendency for pore pressure generation after shear strains greater than the cyclic threshold shear strain have been induced in the instrumented soil mass. Furthermore, they also allow the nonlinear shear modulus behavior of a liquefiable soil deposit to be quantified in terms of induced shear strain amplitude and number of loading cycles using an active in-situ test method.

The in-situ liquefaction testing equipment, field technique and data analysis procedures have been used to conduct field experiments at the Wildlife Liquefaction Array (WLA) in Imperial Valley, California. In-situ tests were conducted in a liquefiable soil deposit approximately 3 to 4 m below the ground surface at three separate locations at WLA. These tests were successful at measuring: (1) excess pore water pressure generation, and (2) nonlinear shear modulus behavior in the native silty-sand deposits as a function of induced cyclic shear strain and number of loading cycles.

The in-situ liquefaction tests conducted at WLA were the first of their kind and show potential for

shedding additional light on the phenomenon of soil liquefaction, despite the practical limitations of widespread use. While this test method may never be applied on a routine basis to evaluate liquefaction potential in a manner similar to the SPT, CPT and  $V_s$  simplified methods, it will eventually be used to directly evaluate the coupled pore pressure response and nonlinear soil behavior of different types of soils (geologic ages, fines contents, plasticities, etc.) under their in-situ conditions (state of stress, saturation level, density, etc.). These in-situ dynamic tests will provide fundamental insight into the potential for various soil deposits to strain, generate pore pressure, degrade in stiffness and subsequently deform further. This information cannot be provided by other routine in-situ test methods. Furthermore, this testing method can be used to evaluate soil improvement techniques (Chang et al. 2004, Rix et al. 2007), and it may also prove useful for generating data sets to refine and validate current numerical models for predicting pore pressure generation and soil softening due to the combined effects of modulus nonlinearity and degradation. These potential future applications will hopefully help lead the profession to deformation-based liquefaction analyses.

While this technique has future potential, it also has some limitations that require further research. Foremost among these is the ability to test soils at greater depths. Thus far, tests have been conducted at a maximum depth of 4 m below the ground surface. To fully characterize potentially liquefiable soil deposits the technique will need to be able to evaluate soils down to at least 15 m. It also appears that the limiting factor for this technique is as much a function of the depth below the surface of the liquefiable layer as it is the absolute depth below the ground surface. Meaning, in order to couple large strains deep into a liquefiable layer from the ground surface the upper portion of that liquefiable layer must also sustain large strains. These strains induce high excess pore pressures, which soften the soil significantly and prevent larger strains from propagating deeper into the layer. Current research is ongoing that will allow energy to be coupled directly to deeper layers.

### **Acknowledgments**

Financial support was provided by the U.S. Geological Survey under grant #04HQGR0073 “Field Evaluation of Liquefaction Resistance at Previous Liquefaction Sites in Southern California.” This support is gratefully acknowledged. This work could not have been conducted without the research tools developed through the George E. Brown, Jr. Network for Earthquake Engineering Simulation (NEES). In particular, the NEES research sites at the University of Texas and the University of California, Santa Barbara were particularly utilized. Dr. T. Leslie Youd, Mr. Min Jae Jung and Mr. Cecil Hoffpauir were instrumental in conducting the field work. Any opinions, conclusions or recommendations expressed in this article are those of the authors and do not necessarily reflect the views of the USGS or NEES.

## References

- Bathe, K. –J. (1996) *Finite Element Procedures*, Prentice-Hall, Inc., NJ. 1037 p.
- Bennett, M.J., McLaughlin, P.V., Sarmiento, J.S. and Youd, T.L. (1984), *Geotechnical Investigation of Liquefaction Sites, Imperial Valley, California, Open File Report 84-252*, Department of the Interior, U.S. Geological Survey, Menlo Park, California.
- Bierschwale, J.G. and Stokoe, K.H., II (1984), *Analytical Evaluation of Liquefaction Potential of Sands Subjected to the 1981 Westmorland Earthquake*, Geotechnical Engineering Report GR 84-15, University of Texas, Austin.
- Chang, W.J. (2002), *Development of an In-Situ Dynamic Liquefaction Test*, Ph.D. Dissertation, The University of Texas, Austin, Texas. 316 p.
- Chang, W.-J., Rathje, E.M., Stokoe II, K.H., and Cox, B.R. 2004. “Evaluation of Effectiveness of Prefabricated Drains in Liquefiable Sand,” *Soil Dynamics and Earthquake Engineering*, 24(9-10), pp. 623-731.
- Chang, W.J., Rathje, E.M., Stokoe, K.H., and Hazirbaba, K. (2007). “In Situ Pore Pressure Generation Behavior of Liquefiable Sand,” *Journal of Geotechnical and Geoenvironmental Engineering*, ASCE (accepted for publication).
- Charlie, W.A., Jacobs, P.J., and Doehring, D.O. (1992) “Blast-induced Liquefaction of an Alluvial Sand Deposti,” *Geotechnical Testing Journal*, Vol. 15, No. 1, pp. 14-23.
- Cook, R.D., Malkus, D.S. and Plesha, M.E. (1989), *Concepts and Applications of Finite Element Analysis, 3<sup>rd</sup> Edition*, John Wiley and Sons, New York, NY.
- Cox, B.R. (2006), *Development of a Direct Test Method for Dynamically Assessing the Liquefaction Resistance of Soils In Situ*, Ph.D. Dissertation, The University of Texas, Austin, Texas. 498 p.
- Dobry, R., Ladd, R.S., Yokel, F.Y., Chung, R.M. and Powell, D. (1982), *Prediction of Pore Water Pressure Buildup and Liquefaction of Sands During Earthquakes by the Cyclic Strain Method*, National Bureau of Standards Building Science Series 138, July, 168 p.

- Dobry, R., Elgamal, A.-W., Baziar, M. and Vucetic, M. (1989), "Pore Pressure and Acceleration Response of Wildlife Site During the 1987 Earthquake," *2<sup>nd</sup> U.S. – Japan Workshop on Soil Liquefaction*, T.D. O'Rourke and M. Hamada, eds. NECEER Report No. 89-0032, Buffalo, N.Y., pp. 145-160.
- Dobry, R., Baziar, M.H., O'Rourke, T.D., Roth, B.L. and Youd, T.L. (1992), "Liquefaction and Ground Failure in the Imperial Valley, Southern California During the 1979, 1981 and 1987 Earthquakes," *Case Studies of Liquefaction and Lifeline Performance During Past Earthquakes*, Vol. 2, Edited by T. O'Rourke and M. Hamada, Feb., Technical Report NCEER-92-0002
- Dunnicliff, J. (1988), *Geotechnical Instrumentation for Monitoring Field Performance*, John Wiley & Sons, Inc., New York, 577 pp.
- Gohl, W.B., Howie, J.A., and Rea, C.E. (2001), "Use of Controlled Detonation of Explosives for Liquefaction Testing," *Proceedings, 4<sup>th</sup> International Conference on Recent Advances in Geotechnical Earthquake Engineering and Soil Dynamics a Symposium in Honor of Professor W.D. Liam Finn*, Paper No. 9.13, San Diego, CA, USA, March 26-31.
- Haag, E.D. and Stokoe, K.H., II (1985), *Laboratory Investigation of Static and Dynamic Properties of Sandy Soils Subjected to the 1981 Westmorland Earthquake*, Research Report GR85-11, Geotechnical Engineering Center, University of Texas, Austin.
- Hardin, B. O. (1978), "The Nature of Stress-Strain Behavior of Soil", *Proc. ASCE Specialty Conference on Earthquake Engineering and Soil Dynamics*, ASCE, New York, N.Y., 3-90.
- Holzer, T. L., Youd, T. L. and Hanks, T. C. (1989), "Dynamics of Liquefaction During the Superstition Hills Earthquake (M=6.5) of November 24,1987," *Science*, 244, April 7: 56-59.
- Hushmand, B., Scott, R.F. and Crouse, C.B. (1992) "In-Situ Calibration of USGS Transducers at Wildlife Liquefaction Site, California, USA," *Proc. 10<sup>th</sup> World Conference on Earthquake Engineering*, A.A. Balkema Publishers, Rotterdam, Netherlands, pp. 1263 – 1268.
- Ishihara, K., Shimizu, K. and Yamada, Y. (1981), "Pore Water Pressure Measured in Sand Deposits During an Earthquake," *Soils and Foundations*, 2(4): 85-100.

- Ishihara, K., Muroi, T. and Towhata, I. (1989), "In-Situ Pore Water Pressure and Ground Motions During the 1987 Chiba-Toho-Oki Earthquake," *Soils and Foundations*, 29(4): 75-90.
- Rathje, E.M., Chang, W.J. and Stokoe, K.H., II (2005), "Development of an In Situ Dynamic Liquefaction Test," *ASTM Geotechnical Testing Journal*, Vol. 28, No. 1, pp. 50-60.
- Rathje, E.M., Chang, W.-J., Stokoe, K.H., II and Cox, B.R. (2004), "Evaluation of Ground Strain from In Situ Dynamic Testing," Paper No. 3099, *13<sup>th</sup> World Conference on Earthquake Engineering*, Vancouver, Canada, August.
- Rix, G., Boulanger, R. Conlee, C., Gallagher, P., Kamai, R., Kano, S., Marinucci, A., and Rathje, E. 2007. "Large-Scale Geotechnical Simulations to Advance Seismic Risk Management for Ports," *4<sup>th</sup> International Conference on Earthquake Geotechnical Engineering*, Thessaloniki, Greece, June (CD-ROM).
- Seed, H.B. and Idriss, I.M. (1970), "Soil Modulus and Damping Factors for Dynamic Response Analysis," *Rep. No. EERC 70-10*, Earthquake Engrg. Res. Ctr., Univ. of California at Berkeley, Calif.
- Seed, H.B. and Idriss, I.M. (1982), *Ground Motion and Soil Liquefaction During Earthquakes*, Earthquake Engineering Research Institute, Berkeley, California, 134 p.
- Shen, C.K., Wang, Z. and Li, X.S. (1991), "Pore Pressure Response During the 1986 Lotung Earthquake," *Proceedings, 2<sup>nd</sup> Int. Conf. on Recent Advances in Geotech. Earthquake Engrg. and Soil Dynamics*, S. Prakash, ed., National Science Foundation, Washington, D.C: 557-563
- Stokoe K.H. II, Rathje, E.M. and Cox, B.R. (2004), "Using Large Hydraulic Shakers to Induce Liquefaction in the Field," *International Conference on Cyclic Behavior of Soils and Liquefaction Phenomena*, Bochum, Germany, March 31– April 2.
- Vucetic, M. and Dobry, R. (1986), "Pore Pressure Build Up and Liquefaction at Level Sandy Sites During Earthquakes," *Research Report*, Department of Civil Engineering, Rensselaer Polytechnic Institute, Troy, New York.

- Youd, T.L. and Bartlett, S.F. (1988), "U.S. Case Histories of Liquefaction-Induced Ground Failure," *Proceedings, First Japan-U.S. Workshop on Liquefaction, Large Ground Deformation, and Their Effects on Lifeline Facilities*, Tokyo, Japan, pp. 22-31.
- Youd, T.L. and Holzer, T.L. (1994), "Piezometer Performance at Wildlife Liquefaction Site, California," *Journal of the Geotechnical Engineering Division*, ASCE, 120(GT6): 975-995.
- Youd, T.L., Idriss, I.M., Andrus, R.D., Arango, I., Castro, G., Christian, J.T., Dobry, R., Finn, W.D.L., Harder, F.L., Jr., Hynes, M.E., Ishihara, K., Koester, J.P., Liao, S.S.C., Marcuson, W.F., III, Martin, G.R., Mitchell, J.K., Moriwaki, Y., Power, M.S., Robertson, P.K., Seed, R.B., and Stokoe, K.H., II (2001), "Liquefaction Resistance of Soils: Summary Report from the 1996 NCEER and 1998 NCEER/NSF Workshops on Evaluation of Liquefaction Resistance of Soils," *ASCE Journal of Geotechnical and Geoenvironmental Engineering*, Vol. 127, No. 10, pp. 817-833.
- Zeghal, M. and Elgamal, A.-W. (1994), "Analysis of Site Liquefaction Using Earthquake Records," *Journal of the Geotechnical Engineering Division*, ASCE, Vol. 120, No. 6, pp. 996-1017.
- Zeghal, M., Elgamal, A.-W., Tang, H.T. and Stepp, J. C. (1995), "Lotung Downhole Array. II: Evaluation of Soil Nonlinear Properties," *Journal of the Geotechnical Engineering Division*, ASCE, Vol. 121, No. 4, pp. 363-378.

## Figure Captions

- Figure 1 (Color online) Cross-sectional schematic layout of triaxial vibroseis truck and trapezoidal liquefaction sensor array used for in-situ dynamic liquefaction tests in native soil deposits.
- Figure 2 (Color online) Schematic detailing the dimensions and components of the in-situ liquefaction sensor.
- Figure 3 (Color online) In-line view of an installed liquefaction sensor array from the ground surface.
- Figure 4 (Color online) Example of a shear strain time history calculated at the center of the in-situ liquefaction sensor array using a 4-node, finite element strain formulation.
- Figure 5 (Color online) Examples of pore pressure time histories obtained during in-situ liquefaction testing in which: a) induced shear strains were not large enough to generate excess pore water pressure, and b) induced shear strains were large enough to generate excess pore water pressure.
- Figure 6 (Color online) Schematic detailing the liquefaction sensor array and the components of particle motion used to calculate the strain dependent shear wave velocity of the instrumented soil mass.
- Figure 7 (Color online) Cycle-by-cycle shear wave velocities from an in-situ liquefaction test with: a) relatively moderate induced shear strains, and b) relatively large induced shear strains.
- Figure 8 (Color online) Example of pore pressure generation curves and nonlinear soil shear modulus values obtained from in-situ dynamic liquefaction tests conducted at the Wildlife Liquefaction Array (WLA).

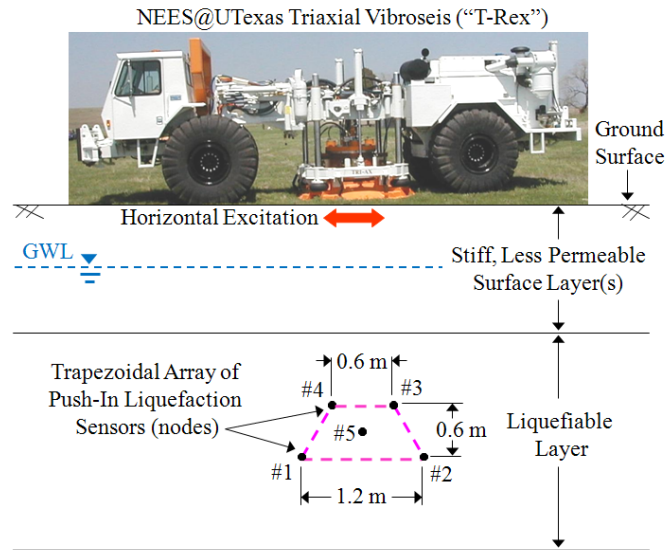


Figure 1

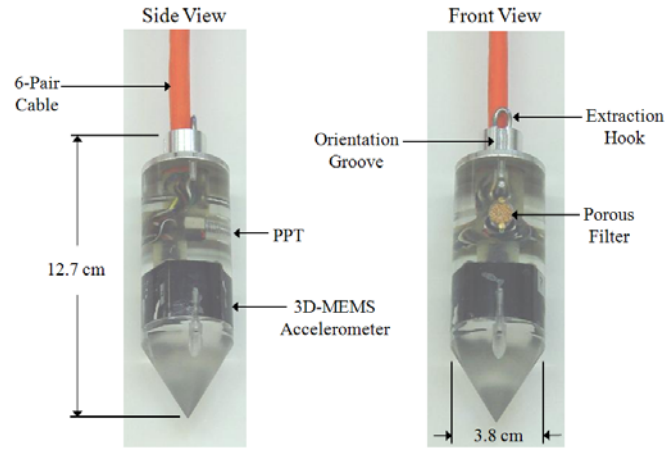


Figure 2

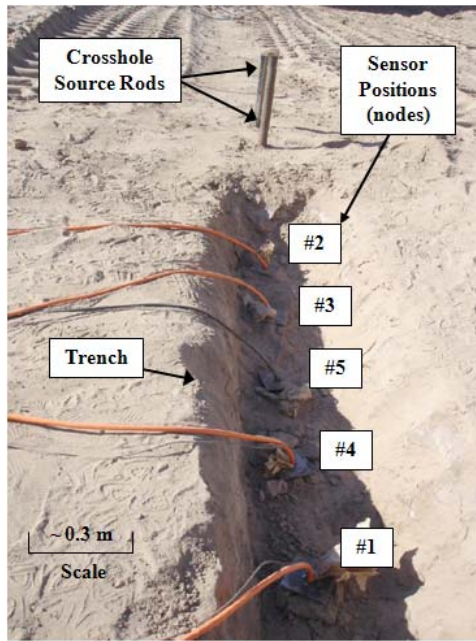


Figure 3

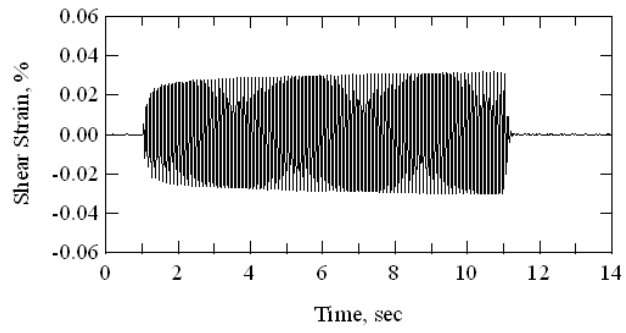


Figure 4

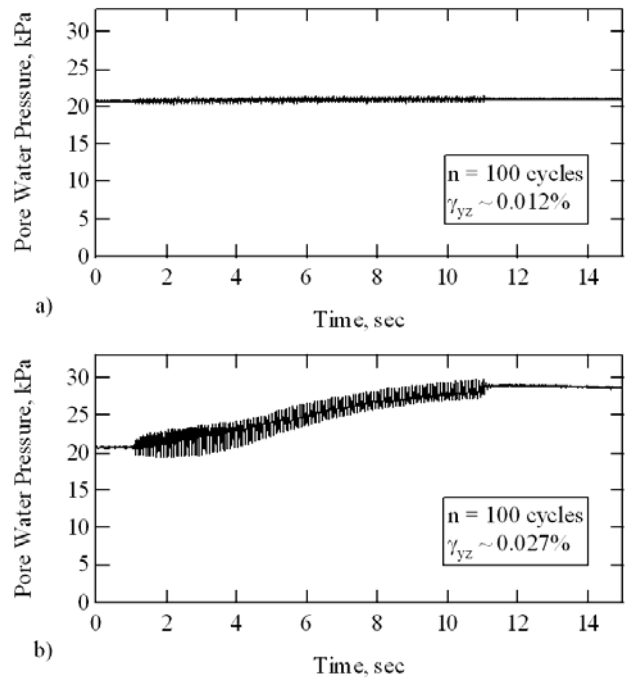


Figure 5

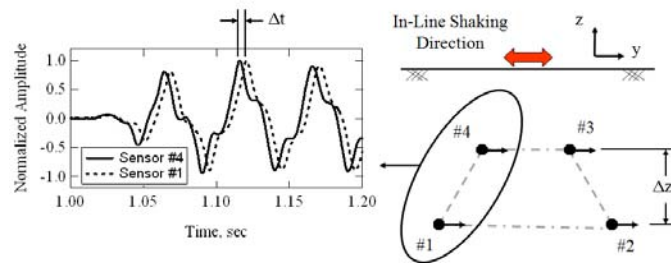


Figure 6

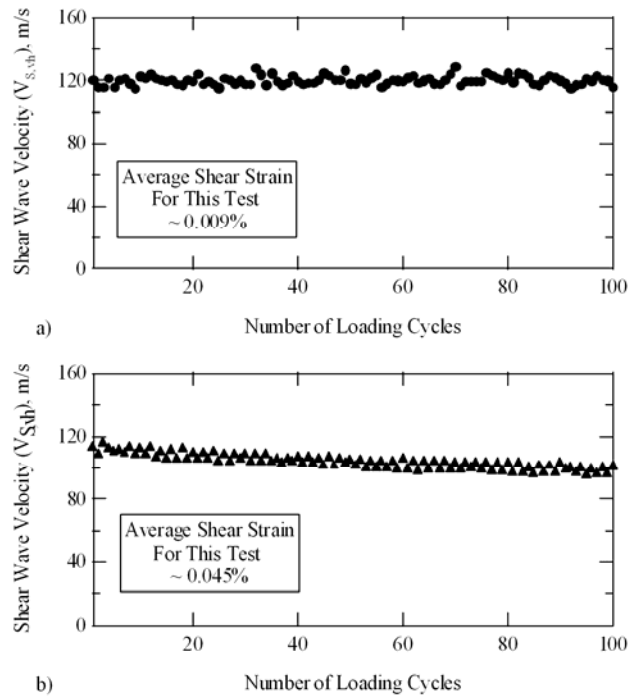


Figure 7

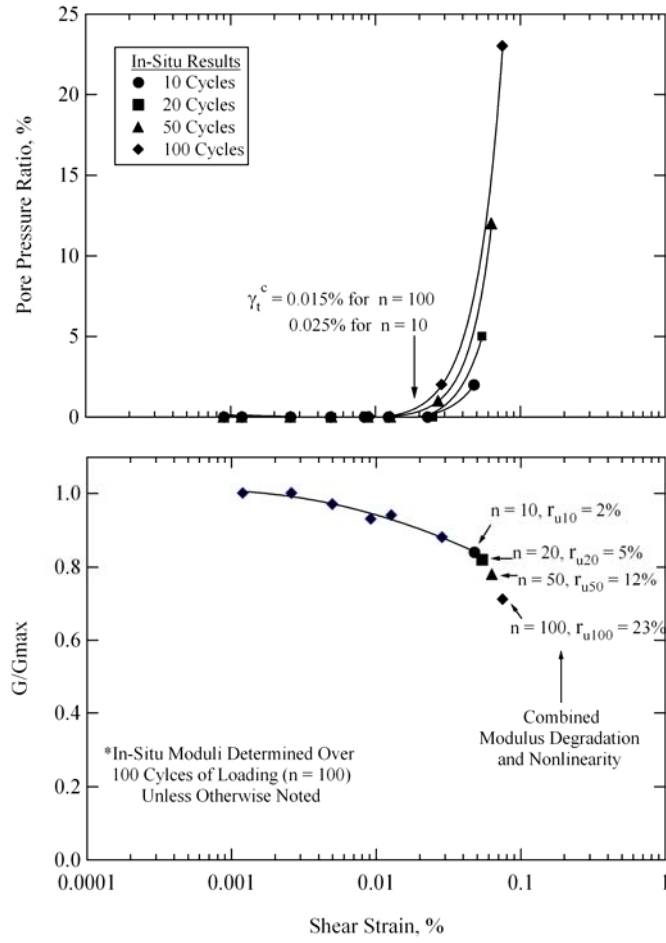


Figure 8